

# 1 Surface and bottom ~~M~~marine heatwave characteristics in the Barents Sea: ~~impact~~ 2 of changing baselines ~~a~~ model study

3 Vidar S. Lien<sup>1\*</sup>, Roshin P. Raj<sup>2</sup>, Sourav Chatterjee<sup>3</sup>

4 <sup>1</sup>Institute of Marine Research, Norway

5 <sup>2</sup>Nansen Environmental and Remote Sensing Center, Norway

6 <sup>3</sup>National Centre for Polar and Ocean Research, Ministry of Earth Sciences, India

7 \*Correspondence to: Vidar S. Lien (vidar.lien@hi.no)

8

9 **Abstract.** Anomalously warm oceanic events, often termed marine heatwaves, can potentially impact the ecosystem in the  
10 affected region and has therefore become a hot topic for research in recent years. Determining the ~~amplitudes-intensity~~ and  
11 ~~spatial~~ extent of marine heatwaves, however, depends on the definition and climatological ~~baseline-average~~ used. Moreover,  
12 the stress applied by the heatwave to the marine ecosystem will depend on which component of the ecosystem is considered.  
13 Here, we utilize a model reanalysis (1991-2024~~2~~) to explore the frequency, ~~intensity-intensity~~, and duration of marine  
14 heatwaves in the Barents Sea, as well as ~~their-regional~~ ~~expression~~~~occurrence-of-MHW~~~~heterogeneities~~. We find that major  
15 marine heatwaves are rather coherent throughout the region, ~~but surface marine heatwaves occur more frequent while~~  
16 ~~heatwaves on the ocean floor have longer duration, and have comparable characteristics near the sea surface and the bottom~~  
17 ~~floor expressions~~. Moreover, we ~~investigate the sensitivity to the choice of utilize a 60-year regional model hindcast to show~~  
18 ~~the impact of changing climatological average length when calculating marine heatwave statistics-baselines-on marine heatwave~~  
19 ~~statistics~~. Our results indicate that severe marine heatwaves ~~are likely~~~~may~~ ~~become~~ more frequent in a future Barents Sea  
20 due to ongoing climate change.

## 21 **1 Introduction**

22 ~~A~~ ~~M~~marine heatwaves (MHW) ~~are~~ ~~s~~ a periods of ~~a~~ warm spells in an ocean region and ~~are~~ ~~s~~ usually defined as ~~a~~ periods when  
23 the temperature exceeds a given threshold ~~based-on~~~~relative to~~ a climatological ~~baseline~~~~average~~ (e.g., Marbá et al., 2015;  
24 Hobday et al., 2016; Scannell et al., 2016; ~~Hu et al., 2020; Huang et al., 2021~~). Due to the potential profound impact on marine  
25 life (e.g., Smale et al., 2019; Husson et al., 2022) and, hence, also socioeconomic impacts (Smith et al., 2021), MHWs have  
26 received increasing attention in recent years, see Oliver et al. (2021) for a comprehensive review of recent literature. While  
27 the criteria to define MHWs seem to converge to those proposed by Hobday et al. (2016), i.e., ~~the~~ temperatures ~~above~~~~exceeding~~  
28 the 90<sup>th</sup> percentile ~~based-on~~ ~~at~~ ~~the~~ ~~moving~~ ~~fixed~~ ~~baseline~~~~climatological~~ ~~average~~, little attention has been given to the impact of  
29 the choice of ~~baseline-period,~~ ~~or~~ ~~climatological~~ ~~average~~ ~~normal~~, on the MHW characteristics and statistics such as frequency,  
30 intensity and duration (Chiswell, 2022). The underlying trends of global ocean warming (e.g., Cheng et al., 2022) and regional

Formatted: Superscript

31 climate variability (e.g., Smedsrud et al., 2022) both impact the MHW statistics, and some regions may eventually enter a state  
32 of permanent MHW, ~~depending on the climatological average chosen when compared with fixed baseline periods~~. As an  
33 example, while Fröhlicher et al. (2018) found a doubling of MHW days between 1982 and 2016 globally, Chiswell (2022)  
34 showed that accounting for climate change by removing the linear trend resulted in weaker MHWs in the tropics and stronger  
35 MHWs in the northern Pacific and Atlantic Oceans.

36  
37 When MHWs are calculated ~~as a timeseries~~ for a whole region, ~~possible~~ regional heterogeneities ~~will~~ may be ~~masked~~ ~~lacking~~,  
38 ~~and~~, thereby reducing the applicability of ~~such using the timeseries as an~~ MHW index. The Barents Sea is a complex shelf sea  
39 that mainly consists of a relatively warm and ice-free Atlantic Water dominated part in the south, and a cold, seasonally ice-  
40 covered Arctic Water dominated part in the north. ~~The southern part is kept ice free by relatively warm and saline Atlantic~~  
41 ~~Water entering to the southwest. The Atlantic Water gives up most of its heat (relative to the average temperature of the Polar~~  
42 ~~Basin) to the atmosphere while en route (e.g., Gammelsrød et al., 2009; Smedsrud et al., 2013). Moreover, the inflow of~~  
43 ~~Atlantic Water has been shown to be a precursor for interannual variability in the Barents Sea sea-ice cover (Onarheim et al.,~~  
44 ~~2015; Schlichtholz, 2019) as well as the ocean heat content further downstream in the Barents Sea (Lien et al., 2017). Moreover,~~  
45 ~~both the southern and northern Barents Sea regions~~ have varying seasonal stratification, ~~mainly from melting of sea ice in~~  
46 ~~the north and solar insolation causing thermal stratification in the south~~ (e.g., Smedsrud et al., 2013; Lind et al., 2018). The  
47 marine ecosystem is ~~therefore also~~ differing between the two main regions, with further diversification within each region.  
48 ~~(see, e.g., Jakobsen and Ozhigin (2011) for a comprehensive overview)~~. However, the extension of the two regimes is changing  
49 due to ongoing climate change, with the boreal, southern part expanding at the expense of the northern, Arctic part (e.g.,  
50 Fossheim et al., 2015; Oziel et al., 2020). The Barents Sea is home to several important, commercial fish stocks, ~~both pelagic~~  
51 ~~(e.g., capelin (*Mallotus villosus*) and Norwegian spring spawning herring (*Clupea harengus*)) and demersal (e.g., northeast~~  
52 ~~Arctic cod (*Gadus morhua*) and haddock (*Melanogrammus aeglefinus*))~~, in addition to a diverse marine ecosystem including  
53 large groups of marine mammals and sea birds ~~as well as unique benthos communities (see Jakobsen and Ozhigin (2011) for~~  
54 ~~a more comprehensive overview)~~. Hence, MHWs may have profound impacts on marine living resources, ~~especially but~~ with  
55 different species exhibiting differences in resilience to MHW events (e.g., Husson et al., 2022). ~~Recent studies on MHWs in~~  
56 ~~the Barents Sea, however, have focused on the surface or the upper parts of the water column (Mohamed et al., 2022; Husson~~  
57 ~~et al., 2022).~~

58 Here, we investigate the occurrences of ~~both~~ surface and bottom MHWs in four contrasting environments in the Barents Sea.  
59 Moreover, we explore the differences in frequency, ~~intensity and duration and intensity based on using~~ varying ~~methodology~~  
60 ~~climatological baseline average lengths~~ for estimating MHWs. We also focus on the ~~most severe~~ ~~highest-intensity~~ MHW event  
61 in terms of cumulative degree-days and investigate its oceanic and atmospheric preconditioning and ~~decay~~ ~~decline~~.

Formatted: Font: Italic

Formatted: Font: Italic

Formatted: Font: Italic

Formatted: Font: Italic

## 62 2 Data & Methods

### 63 2.1 Model data

64 We based our analysis on modeled daily averages from ~~two different models~~; the EU Copernicus Marine Service  
65 ocean reanalysis for the Arctic region based on the TOPAZ model system for the period 1991-2022 (Sakov et al., 2012; Xie  
66 et al., 2016; [Lien et al., 2016](#) product ref 1, Table 1), hereinafter termed *TOPAZ reanalysis*. ~~In addition, we have used a regional  
67 model hindcast utilizing the ROMS model (Regional Ocean Modeling System; Shepetchkin and McWilliams, 2005)  
68 configured for the Nordic and Barents Seas region (Lien et al., 2013, 2014, 2016; product ref 2, Table 1), hereinafter termed  
69 ROMS regional hindcast.~~

70 **Table 1: Products used and their documentation.**

Product ref. no.	Product ID & type	Data access	Documentation
1	ARCTIC_MULTIYEAR_PHY_002_003; Numerical models	EU Copernicus Marine Service Product (2022)	Quality Information Document (QUID): Xie & Bertino (2022) Product User Manual (PUM): Hackett et al. (2022)
<del>2</del>	<del>NordicSeas_4km, Numerical models</del>	<del>MET Norway Thredds Service</del>	<del>Lien et al. (2013, 2014)</del>
<del>23</del>	Conductivity-Temperature-Depth data obtained in the Barents Sea	IMR database TINDOR (data accessible upon request)	
<del>34</del>	ERA5 Gridded Reanalysis (0.25 * 0.25 deg); monthly average on single level	EU Copernicus Climate Service Product (2023)	Hersbach et al., 2023

71

### 72 2.2 Ocean observation data

73 We have used available CTD (*Conductivity-Temperature-Depth*) casts (product ref. ~~32~~, Table 1), covering the period 1986 to  
74 2020, for assessing the performance quality of the ~~two~~ model datasets with regard to bottom temperatures in four regions of  
75 the Barents Sea (Fig. 1) before we use the models results to calculate MHW statistics. The CTD data were obtained from the  
76 Institute of Marine Research database TINDOR (The Integrated Database for Ocean Research).

### 77 2.3 Atmospheric data

78 Monthly averages of turbulent heatfluxes and outgoing longwave radiation [for the period 1993 to 2021](#) were downloaded from  
79 the EU Copernicus Climate Service website (product ref. [34](#), Table 1).

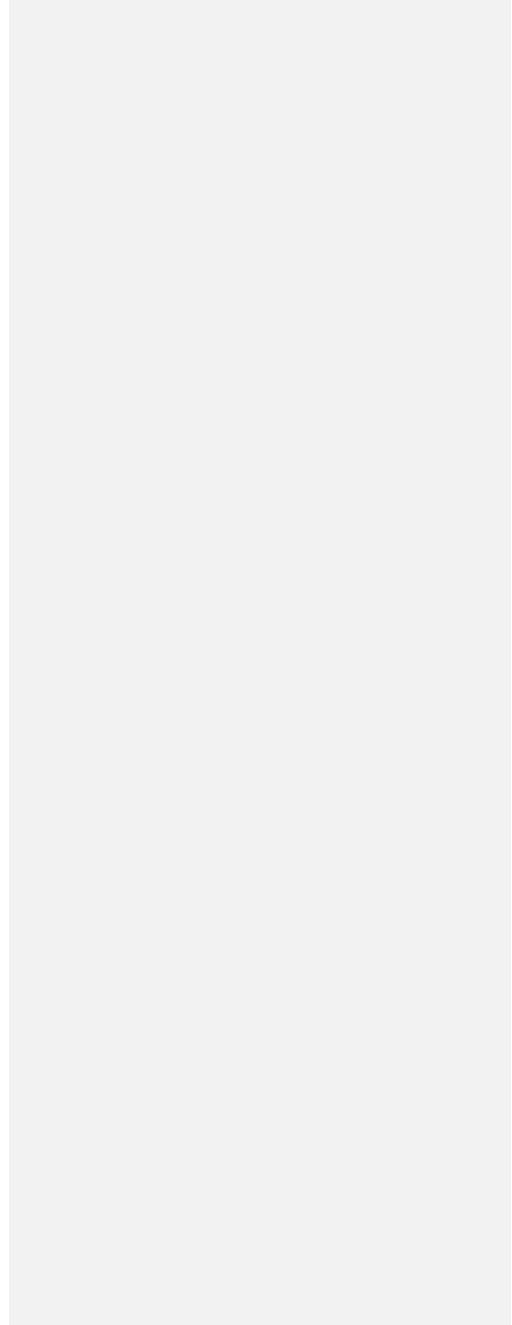
### 80 2.4 Marine heatwave estimation method

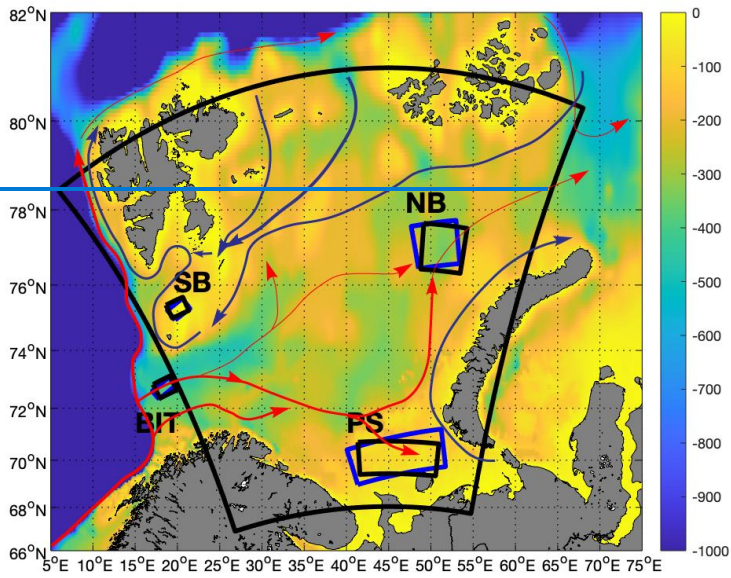
81 We have adopted the definition of MHWs proposed by Hobday et al. (2016), where [an MHWs are-is](#) defined as a period of  
82 more than five days where the temperature is above the [90<sup>th</sup> percentile of the seasonally-daily varying 90<sup>th</sup> percentile threshold](#)  
83 [relative to a predefined baseline climatology averaged over a period at of at](#) least 30 years. Moreover, two consecutive events  
84 divided by a gap of two days or less [isare](#) considered a single event.

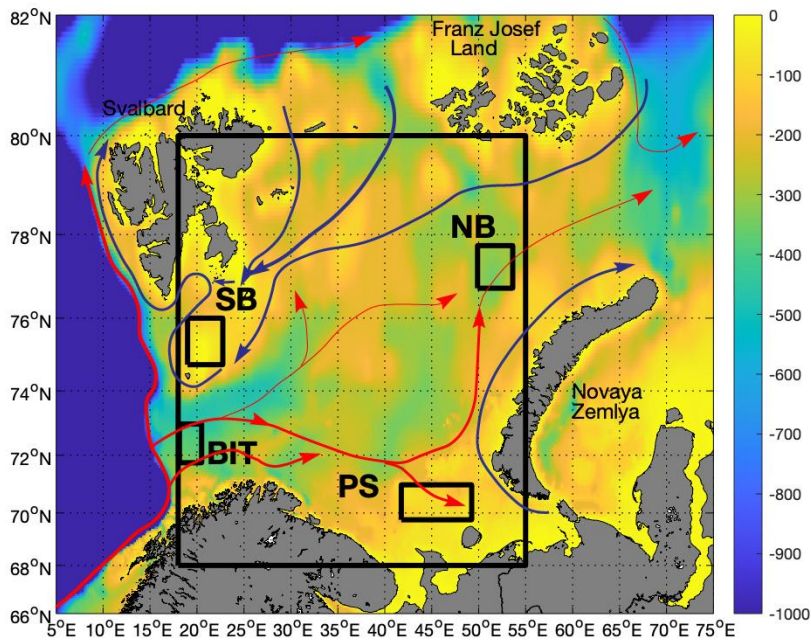
85 The TOPAZ reanalysis covers the time period 1991-2021<sup>2</sup>. In compliance with common standards by the World  
86 Meteorological Organization (WMO 2007; WMO 2015), we have chosen the period 1991-2020 as the climatological [normal](#)  
87 [average period. To study the effect of changing the climatological average period, we have calculated the MHW statistics](#)  
88 [using also the 25-year period 1996-2020 and the 20-year period 2001-2020 as the climatological average periods. For the](#)  
89 [ROMS regional hindcast, which covers the period 1960-2020, we have used two 30-year periods, 1961-1990 and 1991-2020.](#)  
90 [These periods correspond to the previous and most recent, respectively, widely adopted climate normal periods. We choose](#)  
91 [these periods to examine the effect on MHW statistics of using different baseline periods. The first period, 1961-1990, was a](#)  
92 [relatively cold period in the Barents Sea region, whereas the period 1991-2020 has been relatively warm \(e.g., González-Pola](#)  
93 [et al., 2020\).](#)

94 We have chosen four sub-regions where we compute the daily spatially averaged surface and bottom temperatures representing  
95 contrasting marine environments: the Bear Island Trough in the south-western Atlantic Water inflow area to the Barents Sea;  
96 the adjacent Spitsbergen Bank which represents a productive, shallow bank with an Arctic marine environment; the [North-](#)  
97 [eastern Basin in the north-eastern](#) Barents Sea which represents the outflow region where strongly modified Atlantic-derived  
98 water masses leave the Barents Sea; the Pechora Sea to the south-east which represents a shallow and coastal water influenced  
99 area (see map, Fig. 1). Our Bear Island Trough region [falls-is pushed towards the southern slope of the trough outside the full](#)  
100 [Barents Sea region, due to a compromise because of the orientation of the grid, but itto](#) covers the area around 72°30'N [where](#)  
101 [the topography is less complex than further east and which is where the](#) core of the main inflow branch carrying Atlantic Water  
102 to the Barents Sea is located (e.g., Skagseth et al., 2008).

103 For estimating MHW statistics we have used the python package provided by Eric C. J. Oliver:  
104 <https://github.com/ecjoliver/marineHeatWaves> and using the default settings. [Note, that the MHW detection algorithm counts](#)  
105 [every single MHW during a year as a separate event, meaning that a single MHW event that extends over two or more calendar](#)  
106 [years can be counted several times. This will impact the calculation of frequency and the associated trend in occurrences.](#)







109

110 **Figure 1:** Update regions! Map of the Barents Sea. Colors show the bathymetry (in meters). Arrows show the main  
 111 current patterns for Atlantic Water (red) and Arctic Water (blue). Boxes show regions for estimating marine heatwaves  
 112 statistics from the TOPAZ reanalysis (black) and ROMS regional hindcast (blue). BIT: Bear Island Trough; NB:  
 113 nNorth-eastern Barentsin Sea; SB: Spitsbergen Bank; PS: Pechora Sea.

114

#### 115 2.4 Model evaluation

116 Even though both the model products used in this study has previously been evaluated in previous studies against a suite  
 117 of ocean observations (for TOPAZ reanalysis, see: e.g., Lien et al. (2016); Xie et al. (2019, 2023)); for ROMS regional hindcast  
 118 see: Lien et al. (2013, 2014, 2016)). However, because we also used the model for analysis of MHWs near the ocean floor,  
 119 we here provide an assessment of the quality of the model by direct comparison with observations of near-bottom temperature  
 120 from CTD casts where available in the four sub-regions. The motivation for comparing only bottom temperatures is that

Formatted: English (United States)

121 satellite sea surface temperature observations are assimilated into the TOPAZ reanalysis. Moreover, the sea surface  
 122 temperature is also constrained by ocean-atmosphere bulk fluxes. ~~Furthermore, the novelty of our study is the analysis of~~  
 123 ~~MHW events near the ocean bottom, in comparison to previous studies in the Barents Sea focusing mostly on MHW events~~  
 124 ~~at the sea surface or in the upper 50 m of the water column (e.g., Mohamed et al., 2022; Husson et al., 2022).~~

125 ~~Here~~In this model quality assessment, we compared modelled and observed near-bottom temperatures averaged in time  
 126 (monthly) and space (see sub-regions, Fig. 1). The modelled seasonal signal was removed from both model and observation  
 127 timeseries before the correlation was calculated. The comparisons ~~are~~is summarized in Table ~~2~~1 and Supplementary Figure  
 128 S1.

130 **Table 2: Statistics summarizing the comparison between the models and observations at *N* CTD locations. Correlations**  
 131 **are shown in boldface when  $p < 0.05$  and underlined boldface when  $p < 0.01$ . BIT: Bear Island Trough; SB: Spitsbergen**  
 132 **Bank; PS: Pechora Sea; NEBS: North-Easter~~n~~n Barents~~in~~n Sea.**

Model	Statistic	BIT	SB	PS	NEBS
TOPAZ	<i>N</i>	202	49	34	11
	Bias [°C]	1.9	-2.1	-0.8	-0.6
	RMSd [°C]	2.0	2.4	1.0	0.7
	Correlation [ <i>r</i> ]	<b><u>0.55</u></b>	<b><u>0.39</u></b>	<b><u>0.78</u></b>	<b><u>0.66</u></b>

133  
134

### 135 3 Results

136 We first ~~estimate-calculated the~~ MHW statistics based on the TOPAZ reanalysis for the full Barents Sea region for the period  
 137 1991-2022 (see Fig. 1 for area definition), ~~which - Among the MHWs identified, Two distinct MHW events are identified~~  
 138 ~~distinguished both in terms of intensity and duration in both the surface and bottom temperature time series. While the strongest~~  
 139 ~~MHW, in terms of cumulative effect (degree days), appeared in 2016 both near the surface and near the bottom, the second~~  
 140 ~~strongest MHW appeared in 2013 near the surface and in 2012 near the bottom (see Supplementary Figures S2 and S3 for the~~  
 141 ~~full timeseries). When applying the MHW definition provided by Hobday et al. (2016), we computed (The following computed~~  
 142 ~~MHW statistics (are summarized in figure 2 and Tables 3-5). A total of 29 MHWs were identified at the surface compared to~~  
 143 ~~5 MHWs near the bottom, equating to a frequency of 0.90 year<sup>-1</sup> at the surface and 0.16 year<sup>-1</sup> near the bottom. The average~~  
 144 ~~maximum intensity was 1.41 °C and 1.07 °C at the surface and near the bottom, respectively. The duration was, on average,~~

Formatted: Not Highlight  
 Formatted: Not Highlight  
 Formatted: Not Highlight  
 Formatted: Not Highlight



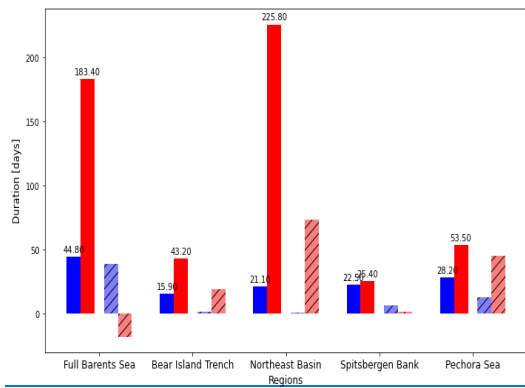
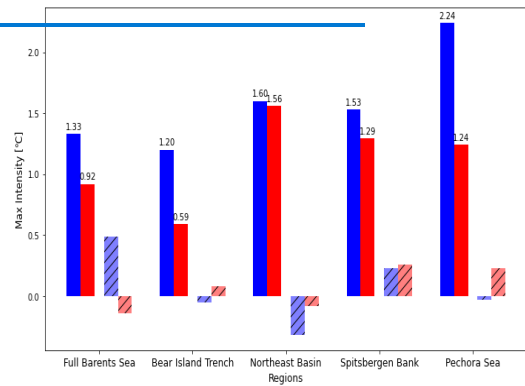
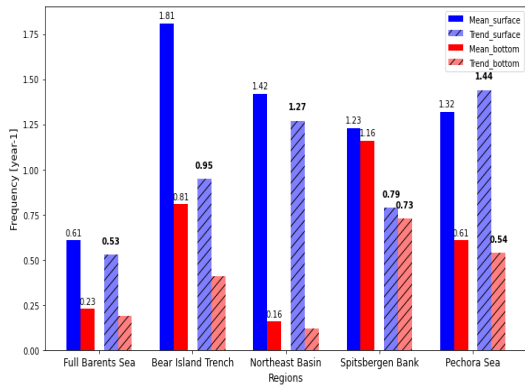
145 longer near the bottom (214 days) than at the surface (33 days). Moreover, we found a positive, decadal trend in the MHW  
146 frequency at the surface of  $0.82 \text{ year}^{-1}$  ( $p < 0.05$ ), while for all the other metrics mentioned above, the decadal trends were non-  
147 significant.

148 Two periods are distinguished in terms of MHW cumulative intensity ( $^{\circ}\text{C days}$ ), both at the surface and near the bottom. The  
149 strongest MHW in the Barents Sea as a whole, in terms of cumulative intensity, occurred in 2016 both at the surface and near  
150 the bottom (Fig. 3a,f). At the surface, the 2016 MHW had an average intensity of  $1.29 \text{ }^{\circ}\text{C}$  (maximum of  $3.41 \text{ }^{\circ}\text{C}$ ) and a total  
151 duration of 480 days (from December 19, 2015, to April 11, 2017). Near the bottom, the 2016 MHW had an average intensity  
152 of  $1.10 \text{ }^{\circ}\text{C}$  (maximum of  $1.28 \text{ }^{\circ}\text{C}$ ) and a total duration of 479 days (February 28, 2016, to June 20, 2017). The second strongest  
153 MHW in terms of cumulative intensity in the Barents Sea as a whole, occurred in 2013 at the surface and in 2012 near the  
154 bottom (see Supplementary Figure S2). While an investigation on possible mechanisms for the decoupling between the surface  
155 and the bottom is beyond the scope of this work, we note that the 2012/13 MHW event was preceded by an extraordinarily  
156 large temperature anomaly but close to average volume transport in the Atlantic Water entering the Barents Sea to the  
157 southwest (e.g., ICES, 2022), as opposed to extraordinarily large volume transports preceding the 2016 MHW event (see below  
158 for more details). Moreover, previous studies have suggested that temperature anomalies that are advected into the Barents  
159 Sea at depth during the stratified summer season, can reemerge at the surface further downstream through vertical mixing  
160 during the following winter (e.g., Schlichtholz, 2019).

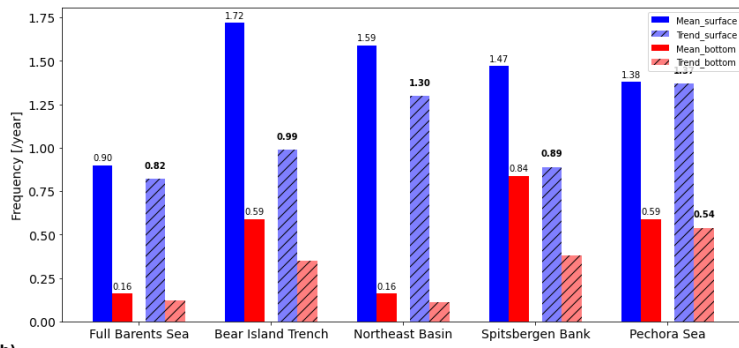
161 Near the surface, the 2016 MHW had an average intensity of  $1.25 \text{ }^{\circ}\text{C}$  above the climatological temperature average  
162 temperature and a total duration of 512 days (from November 18, 2015, to April 12, 2017). Near the bottom, the MHW  
163 expression had an average intensity of  $1.02 \text{ }^{\circ}\text{C}$  above the climatological temperature and a total duration of 587 days (December  
164 30, 2015, to August 7, 2017). However, while the MHW statistics at the surface and near the bottom expression of were  
165 comparable in the 2016 MHW event are comparable, we find some differences between the surface and the bottom when  
166 comparing the MHW statistics between the average surface and bottom expressions of MHW in the Barents Sea in general.  
167 The frequency of MHWs for the 1991–2021 period was found to be  $0.61 \text{ year}^{-1}$  near the surface and  $0.23 \text{ year}^{-1}$  near the  
168 bottom, while the average maximum intensity was found to be  $1.33 \text{ }^{\circ}\text{C}$  and  $0.92 \text{ }^{\circ}\text{C}$  near the surface and bottom, respectively.  
169 The duration was, on average, longer near the bottom (183 days) compared with near the surface (45 days). The frequency and  
170 maximum intensity had positive trends both near the surface and near the bottom, while the duration had a positive trend near  
171 the surface and a negative trend near the bottom. However, these statistics need to be interpreted with care. For example, while  
172 we identified two main MHW events, several shorter periods were also classified as MHWs, especially within the near-bottom  
173 (Supplementary Figures S4a, S5a). Some of these events were related to the same warm period but with intermittent periods  
174 with temperatures below the 90<sup>th</sup> percentile in between. These shorter periods affected the calculation of the duration trend.  
175 Thus, although all the near-bottom MHW events detected occurred within the last 18 years of the 1991–2021 period, no  
176 significant trends were detected in the average duration appeared with a negative trend in the calculations.

Formatted: Not Highlight

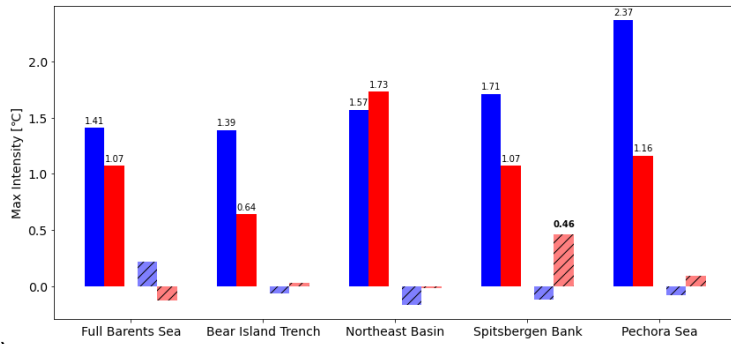
Formatted: Not Highlight



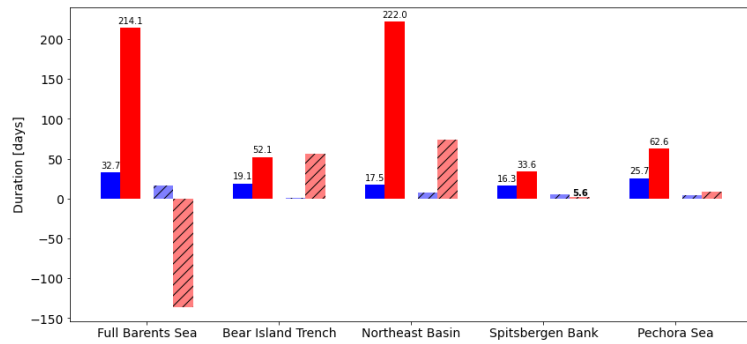
(a)



(b)



(c)



180 **Figure 2: Marine heatwave statistics for the full Barents Sea for the period 1991-2022, using 1991-2020 as the climate**  
181 **average period. a) Number of marine heatwave events per year (top); b) maximum intensity of the heatwave events**  
182 **(middle); c) and average marine heatwave duration (bottom) for the full Barents Sea and four sub-regions during the**  
183 **period 1991-2021. The associated decadal trends are shown in hatched colors. The trend is provided in boldface if**  
184 **significant to 95% ( $p < 0.05$ ). Surface values are shown by blue bars and bottom values are shown by red bars. Based**  
185 **on data from the TOPAZ reanalysis.**

186 To look for investigate possible regional differences heterogeneity in MHWs within the Barents Sea, we chose to  
187 investigate calculated the 2016 MHW statistic event, which was the most severe MHW event detected in the Barents Sea as a  
188 whole, in the four sub-regions depicted in figure 1. The results are summarized in Table 3, 4, and 5. In all regions, we found  
189 a higher frequency of MHW events than for the Barents Sea as a whole (except for near the bottom in the Northeast Basin).  
190 Moreover, all regions showed a larger, positive decadal trend in the frequency compared with the Barents Sea as a whole,  
191 although near the bottom only the trend in the Pechora Sea was found to be statistically significant ( $p < 0.05$ ; Table 3). For the  
192 average maximum intensity, at the surface, we found that the Bear Island Trough, which is the upstream inflow region, had  
193 similar statistics as for the Barents Sea as a whole, while for the other three regions the intensity was generally larger (Table  
194 4). Near the bottom, the intensity in the Bear Island Trough was less than that of the Barents Sea as a whole, while in the  
195 downstream Northeast Basin the intensity was larger on average. In the two other regions the differences were smaller. In  
196 terms of duration, all the regions experienced shorter MHWs on average compared to the Barents Sea as a whole, and especially  
197 so near the bottom. The exception was the Northeast Basin, where the average duration of near-bottom MHWs was found to  
198 be comparable to that of the Barents Sea as a whole (Table 5).

199 To investigate further regional heterogeneity, we considered the MHW event in 2016 in each of the regions. At the surface, in  
200 the TOPAZ reanalysis, the 2016 MHW event was the most severe MHW event in terms of cumulative intensity during the  
201 full 1991-2021 period in three out of the four sub-regions investigated. The exception was the Bear Island Trough, where  
202 the 2012 MHW event was more severe (not shown); the Northeast Basin, the Spitsbergen Bank, and the Pechora Sea. Near  
203 the bottom, in the 2016 MHW event was the most severe MHW event in all four regions the Bear Island Trough, the temperature  
204 anomaly classified as an MHW intermittently throughout 2016 and while the cumulative impact intensity in terms of degree  
205 days was largest in 2016 (at the surface; Supp. Fig. S4b3), 2012 experienced the most severe continuous MHW (Fig. 3, 4).  
206 The progression of the 2016 MHW event was comparable in all regions, except for the Spitsbergen Bank where the onset of  
207 the MHW occurred later, near mid-summer, compared to the other regions where the onset occurred during late winter.  
208 However, on the Spitsbergen Bank the 2016 MHW was preceded by several but less intense and intermittent MHWs. It is also  
209 worth noting that the onset in the other three regions, as well as the Barents Sea as a whole, occurred in late February/early  
210 March, except for in the upstream Bear Island Trough where the onset occurred in the beginning of April. Moreover, both the  
211 average and maximum MHW intensity was less in the Bear Island Trough compared to the other regions. Other regional

Formatted: Font: Not Italic

Formatted: Font: Not Italic

Formatted: Not Highlight

Formatted: Not Highlight

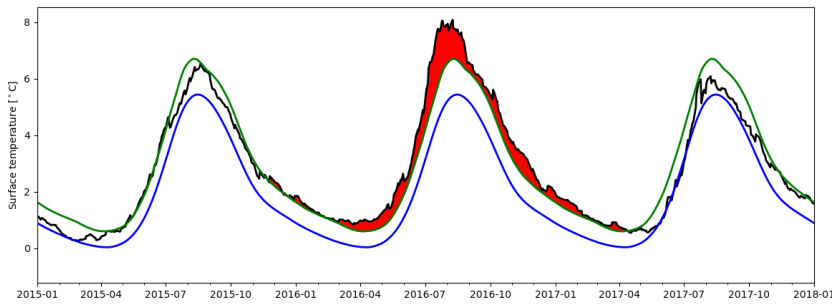
212 differences include that in the downstream north-eastern Barents Sea, the surface expression of the 2016 MHW was most  
213 severe in the first half of 2016, while on the Spitsbergen Bank it was most pronounced in the second half of 2016 (Fig. 4). In  
214 the Pechora Sea, the 2016 MHW persisted throughout the whole year. Moreover, the intensity of the MHW increased  
215 downstream in the Barents Sea, from an average 1.21 °C and 0.60 °C above the climatology near the surface and bottom,  
216 respectively, during the most severe part of the 2016 MHW event in the Bear Island Trough, to 1.54 °C and 1.68 °C,  
217 respectively, in the north-eastern Barents Sea and 2.45 °C and 1.51 °C, respectively, in the Pechora Sea. On the Spitsbergen  
218 Bank, the average intensity was 2.28 °C near the surface and 2.25 °C near the bottom.

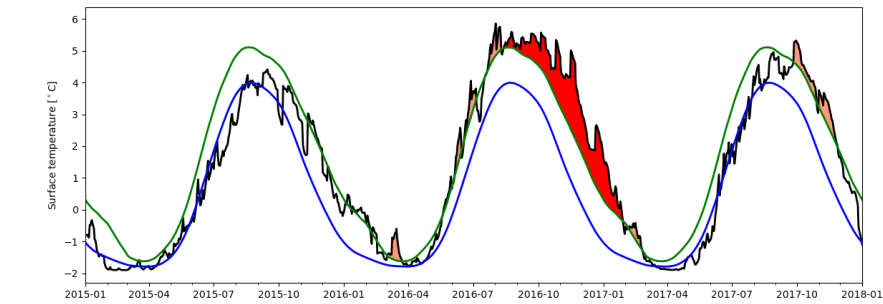
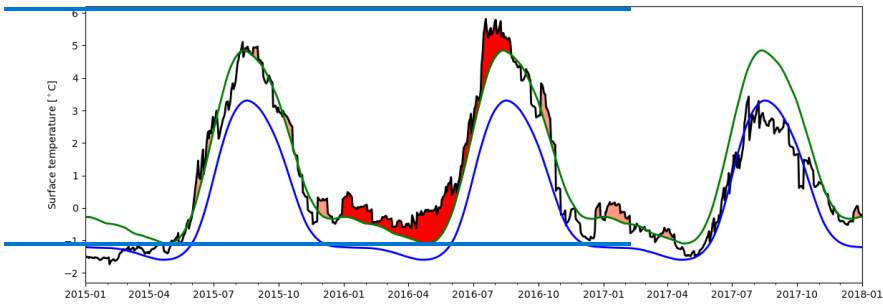
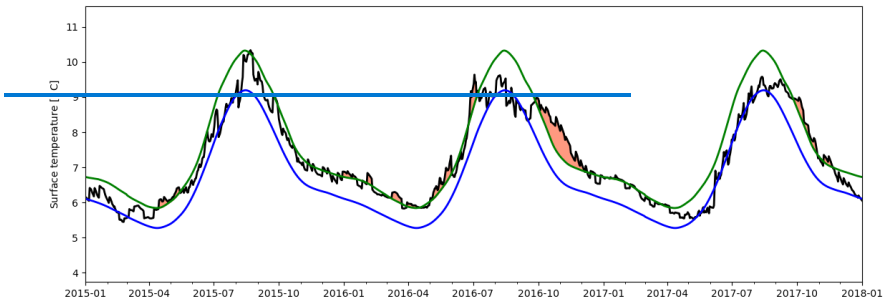
219 In all the sub-regions, except for the Spitsbergen Bank where the water column is well-mixed due to tidal mixing, the frequency  
220 of MHWs frequency is was larger near the surface than near the bottom (Fig. 2a). In the Bear Island Trench and the Pechora  
221 Sea, the maximum intensities of the MHWs near the surface were approximately about twice as large as the maximum  
222 intensities near the bottom, whereas in the north-eastern Barents Sea and on the Spitsbergen Bank the intensities are similar  
223 near the surface and bottom (Fig. 2b). However, the MHWs near the bottom tend to be more persistent, as seen from the longer  
224 average duration (again, the Spitsbergen Bank is an exception; Fig. 2c).

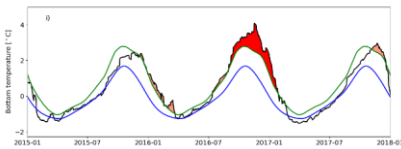
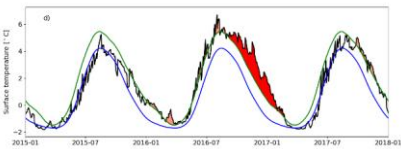
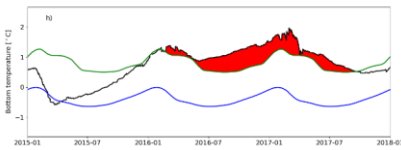
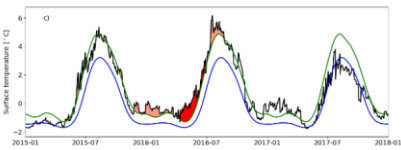
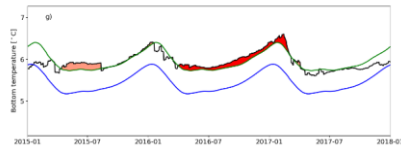
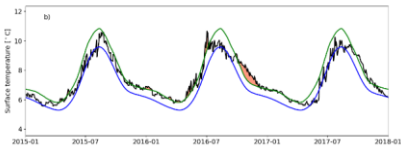
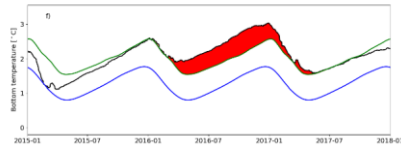
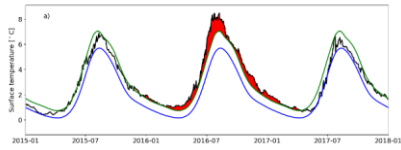
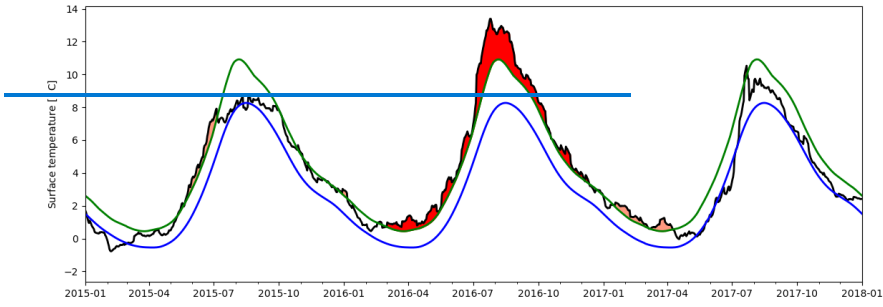
225

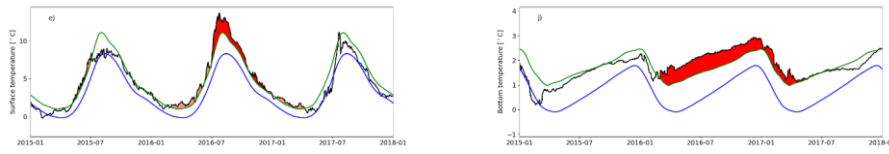
Formatted: Highlight  
Formatted: Space Before: 12 pt, After: 6 pt

Formatted Table

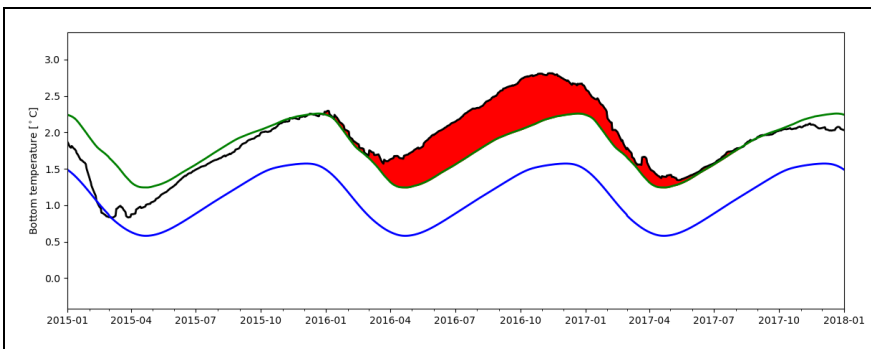




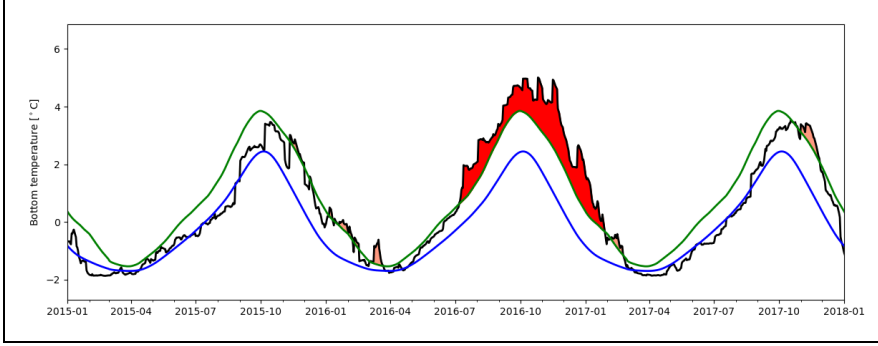
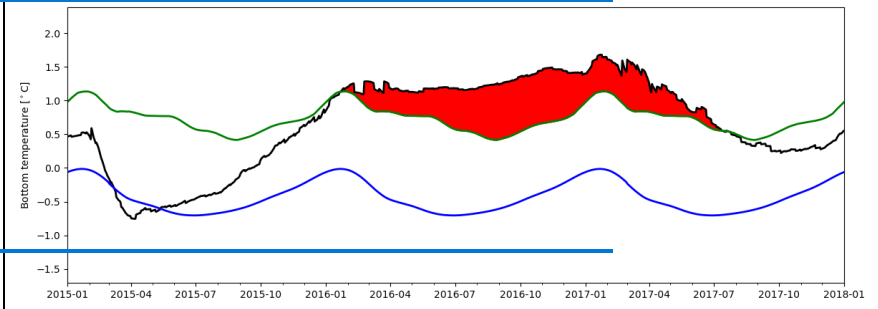
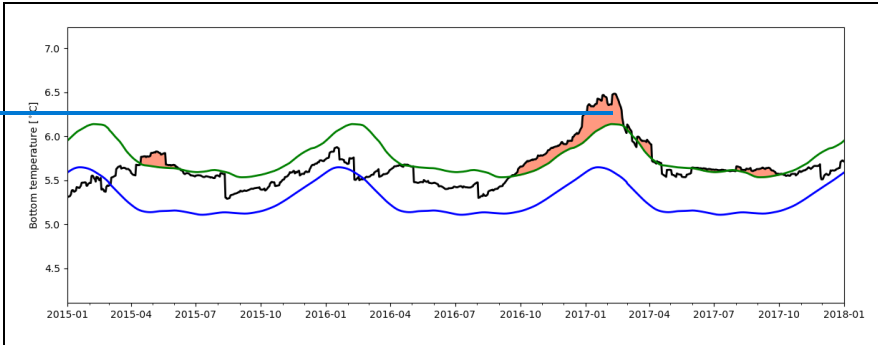




226  
 227 **Figure 3: (Top)** Time series (2015-2017; black lines) showing the temperature at 5-meter depth the surface (left column)  
 228 and near the bottom (right column) spatially averaged over the Barents Sea. Blue lines show daily climatology. Green  
 229 lines show the upper 90th percentile. The highestmost intensity marine heatwave in terms of cumulative degree days  
 230 for the full 1991-2021 period is shown in dark red shading. Other marine heatwaves are shown in pink shading. a) the  
 231 full Barents Sea, surface; b) Subpanels show the following sub-regions (from top to bottom): the Bear Island Trough,  
 232 surface; c) the North-eastern Barents Sea, surface; d) the Spitsbergen Bank, surface; e) the Pechora Sea,  
 233 surface; f) the full Barents Sea, bottom; g) the Bear Island Trough, bottom; h) the Northeast Basin, bottom; i) the  
 234 Spitsbergen Bank, bottom; j) the Pechora Sea, bottom. All panels show the period January 1st 2015 to January 1st  
 235 2018. Note the different scales on the y-axes.







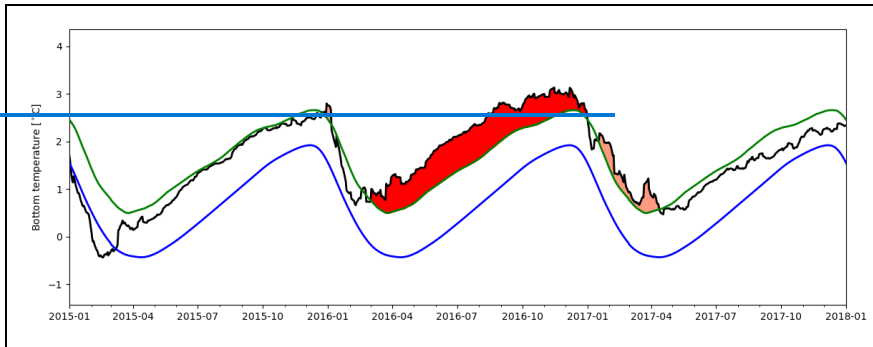


Figure 4: Same as Figure 3, but showing near-bottom temperatures.

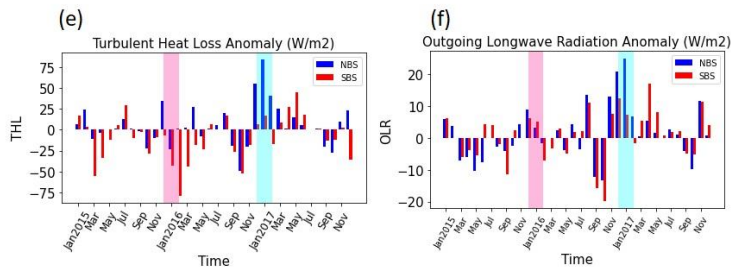
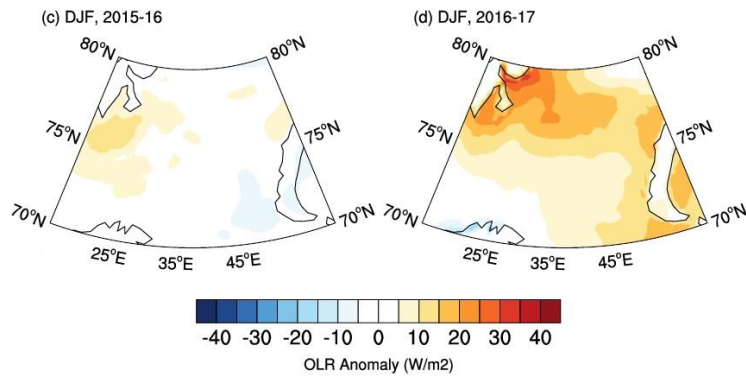
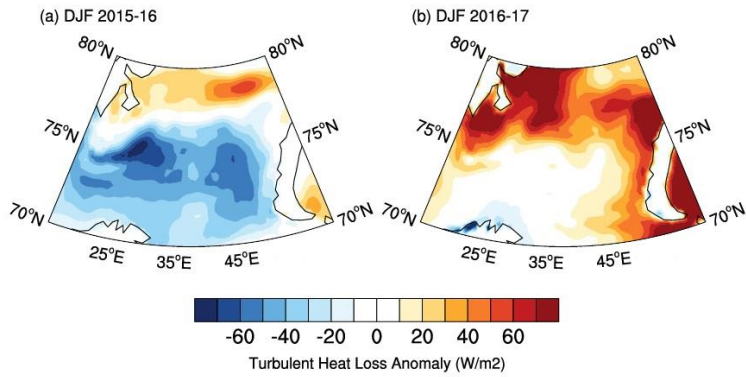
### 3.1 Preconditioning and atmospheric forcing of 2016 MHW event

Leading up to the onset of the 2016 MHW, the inflow of warm Atlantic Water to the Barents Sea was above average during the whole of 2015 (ICES, 2022). However, during the subsequent following winter of 2015/16, the turbulent (latent and sensible) heat loss, however, (was between 20 and 70  $\text{W}/\text{m}^2$  below the 1993-2021 average in the southern Barents Sea (25-45E; 71-75N; i.e., along the Atlantic Water pathway through the Barents Sea; Fig. 4a)), which was below the lowest climatological average for the period (1993-2021) in the southern Barents Sea. The reduced heat loss to the atmosphere occurred (i.e., along the Atlantic Water pathway through the Barents Sea) despite the preceding increased in advection of oceanic heat (Fig. 54a,e). Note, that during the winter months, the solar radiation can be neglected due to the Polar Night conditions in the Barents Sea region. Moreover, wind-driven mixing during winter breaks down the upper water column stratification, connecting the surface with the deeper layers. Furthermore, for the analysis period (1993-2021), the area-averaged turbulent (latent and sensible) heat loss in the southern Barents Sea (25-45E; 71-75N) was also the lowest during the onset of the 2016 MHW event (not shown). Thus, the 2016 MHW event was preceded by an increased Atlantic Water heat transport and reduced heat loss to the atmosphere resulted in the development of this strong MHW event during 2016. While we did not perform a closed heat budget calculation, we note that the oceanic heat carried by the downstream outflow from the Barents Sea has previously been reported to be smaller than the inflow by an order of magnitude (e.g., Gammelsrød et al., 2009; Smedsrud et al., 2013), and that a previous study found that increased oceanic heat advection to the Barents Sea lead to increased ocean heat content in the interior Barents Sea (Lien et al., 2017).

In the following winter of 2016/17, i.e., during the decay line of the 2016 MHW event, the turbulent heat loss and outgoing longwave radiation in the northern Barents Sea (25:45E; 76-80N; Fig. 54b,e,f) reached the largest values in the 1993-2021 period. This was, possibly due to likely enhanced by a record low winter sea ice extent (ICES, 2022) and negative cloud cover

Formatted: Superscript

260 anomaly in the northern Barents Sea (not shown). ~~However,~~ in the southern Barents Sea, however, no ~~obvious changes in~~  
261 heat loss anomaly ~~at from~~ the ocean surface ~~was~~ observed during the winter 2016/17 (Fig. 45b). ~~Rather, the decay of the~~  
262 ~~MHW event in the southern Barents Sea appears to be caused by the decrease in~~ but the Atlantic Water transport ~~aeros~~ through  
263 the Barents Sea Opening decreased during 2016 (ICES, 2022). Thus, the ~~onset and decay of the~~ 2016 MHW event in the  
264 Barents Sea can be linked to the combined influence-effect of increased Atlantic water transport into the Barents Sea, as well  
265 ~~as and~~ reduced oceanic heat loss in the southern Barents Sea during the onset and increased oceanic heat loss ~~and in the~~  
266 northern Barents Sea during the decline.



268 **Figure 45:** Atmospheric preconditioning leading up to the MHW depicted in Fig. 32. (a,b) DJF (December(-1), January,  
269 February (0)) turbulent (latent + sensible) heat loss anomaly (W/m<sup>2</sup>) for 2016 (a) and 2017 (b). Same as (a,b) but for  
270 **Outgoing Longwave Radiation (OLR)**. Positive values indicate upward fluxes. Monthly mean turbulent heat loss (c)  
271 and OLR (f) over northern (blue, 25-45E; 76-80N) and southern (red, 25-45E; 71-75N) Barents Sea. The onset (DJF,  
272 2015-16) and decay (DJF, 2016-17) phase of the 2016 MHW event are shaded in pink and cyan colours. Data: ERA5  
273

### 274 3.2 Effect of changing baselines

275 Next, we investigated the effect of changing the [baseline-climatological average period from 30 years \(1991-2020\) to 25 years](#)  
276 [\(1996-2020\) and 20 years \(2001-2020\)](#) when calculating the MHW statistics [for both the surface and the bottom \(Tables 3-5\)](#);  
277 [using the results from the ROMS regional hindcast. Common for all the four sub-regions is that the frequency of MHW](#)  
278 [occurrences decreased by approximately one half \(two thirds in the north-eastern Barents Sea\) when changing the baseline](#)  
279 [from the 1961-1990 climate normal to the 1991-2020 climate normal \(Table 3\). On the other hand, the decadal trend in the](#)  
280 [number of occurrences not only increased, but are also statistically significant to the 95% level \( \$p < 0.05\$ \) in all regions.](#)  
281 [Oppositely to the frequency, the average maximum intensity was comparable when using the two different baselines in most](#)  
282 [of the sub-regions \(Table 4\). As an exception, in the Pechora Sea, the average intensity increased, especially near the surface,](#)  
283 [when using the 1991-2020 climate normal as baseline. The explanation for the increase in maximum intensity when comparing](#)  
284 [with a higher climatological average temperature is that several weaker warm events were no longer classified as MHW \(not](#)  
285 [shown\).](#)

286  
287 [For all regions, including the Barents Sea as a whole, we found that the frequency of surface MHWs decreased with decreasing](#)  
288 [length of the climatological average period. For near-bottom MHWs, the results were less clear except for a decrease in](#)  
289 [frequency in the two shallow bank regions \(the Spitsbergen Bank and the Pechora Sea\). Similarly, for the intensity at the](#)  
290 [surface, there was a general trend of decreasing average intensity with decreasing length of the climatological average period.](#)  
291 [There was also a trend of decreasing intensities near the bottom, except for in the two shallow bank regions. As opposed to the](#)  
292 [average frequency and intensity, the average duration seemed less dependent on the length of the climatological average period.](#)  
293 [Near the bottom, however, the duration was sensitive to the climatological average period length due to the low number of](#)  
294 [MHWs and the dominance of the 2012 and 2016 MHW events. On average, the MHW duration decreases when changing the](#)  
295 [baseline from the 1961-1990 climate normal to the 1991-2020 climate normal, although the differences are small in the Bear](#)  
296 [Island Trough and on the Spitsbergen Bank \(both in the western Barents Sea; Table 5\). A striking difference between the two](#)  
297 [western sub-regions and the two eastern sub-regions is the transition from more well-mixed condition to more of a stratified](#)  
298 [two-layer system, causing a decoupling between the surface and bottom conditions. As a result, near-bottom MHW show](#)

considerably longer duration than surface MHW in the north-eastern Barents Sea and in the Pechora Sea, whereas in the Bear Island Trough and on the Spitsbergen Bank the duration near the surface and near the bottom are comparable. Indeed, when using 1961-1990 as the baseline in the north-eastern Barents Sea, the most severe MHW in terms of cumulative degree days appears at the end of the 60-year period with the last five years (starting March 10, 2015) of the timeseries representing an MHW (not shown). Thus, the area has entered a state of permanent MHW when choosing this older baseline, which explains the strongly positive trend in duration (129 days per decade; Table 5). Moreover, several MHW events appear throughout the 60-year period, including one MHW event at the start of the timeseries in 1961 (not shown). When the baseline is changed to the 1991-2020 period, two distinct MHW appear, in 2016 and 2018, with the 2016 event being the most severe and no MHW event is detected prior to 2007.

**Table 3: Number-Average frequency of marine heatwaves events per year during the period 1961-2020 +/- the decadal trend for two different baseline periods, 1961-1990 and 1991-2020. The baseline period 1991-2020 is also used for the detrended, full time series (1961-2020). The trend is provided in boldface if significant to 95% ( $p < 0.05$ ), or in italics if not significant ( $p > 0.05$ ). Values for the surface are shown on top and values for bottom are shown below. BIT: Bear Island Trough; SB: Spitsbergen Bank; PS: Pechora Sea; NEBS: North-Eastera Barentsin-Sea.**

Baseline \ Area	<b>FULL</b>	BIT	SB	PS	NEBS
1961-1990	$0.90 + 0.82$ $0.16 + 0.12$	$21.3072 + 0.299$ $20.159 + 0.0635$	$1.473 + 0.2089$ $10.7084 + 0.2238$	$1.38 + 0.14637$ $0.592 + 0.1354$	$1.859 + 0.12930$ $0.163 + 0.11$
1991-2020	$0.84 + 0.85$ $0.44 + 0.18$	$01.953 + 0.3190$ $0.590 + 0.2839$	$01.8216 + 0.2178$ $0.801 + 0.1944$	$01.5709 + 0.12210$ $0.523 + 0.2247$	$01.6344 + 0.1336$ $0.2231 + 0.219$
2001-2020	$0.59 + 0.66$ $0.19 + 0.14$	$1.19 + 0.64$ $0.53 + 0.37$	$1.09 + 0.82$ $0.59 + 0.35$	$0.84 + 0.89$ $0.25 + 0.23$	$1.28 + 1.22$ $0.25 + 0.24$

**Table 4: Same as Table 4, but3 but showing average maximum intensity (in °C).**

Reference period \ Area	<b>FULL</b>	BIT	SB	PS	NEBS
1961-1990	$1.41 + 0.22$ $1.07 - 0.13$	$1.392 + 0.057$ $10.3864 + 0.043$	$1.2710 + 0.0412$ $1.0722 + 0.0346$	$21.373 + 0.208$ $1.316 + 0.079$	$1.0857 + 0.167$ $01.6273 + 0.092$
1991-2020	$1.35 + 0.23$	$1.395 + 0.025$	$1.5726 + 0.107$	$2.3022 + 0.0849$	$1.4758 - 0.285$

Formatted Table

Formatted: Font: Bold, Not Italic

Formatted: Font: Not Bold, Italic

Formatted: Font: Bold, Not Italic

Formatted: Font: Bold, Not Italic

Formatted: Font: Not Bold, Italic

Formatted: Font: Not Bold, Italic

Formatted: Font: Not Bold, Italic

Formatted: Font: Not Bold, Italic

Formatted: Font: Not Bold, Italic

Formatted: Font: Not Bold, Italic

Formatted: Font: Not Bold, Italic

Formatted: Font: Not Bold, Italic

Formatted: Font: Not Bold, Italic

Formatted Table

Formatted: Font: Not Bold, Italic

Formatted: Font: Not Bold, Italic

Formatted: Font: Not Bold, Italic

Formatted: Font: Not Bold, Italic

Formatted: Font: Bold, Not Italic

Formatted: Font: Not Bold, Italic

Formatted: Font: Not Bold, Italic

Formatted: Font: Not Bold, Italic

Formatted: Font: Not Bold, Italic

Reference period \ Area	<b>FULL</b>	<b>BIT</b>	<b>SB</b>	<b>PS</b>	<b>NEBS</b>
	$0.96 + 0.17$	$10.561 + 0.051$	$1.2617 + 0.1058$	$1.5416 + 0.053$	$01.7148 + 0.1067$
2001 - 2020	$1.26 + 0.32$ $0.85 + 0.06$	$1.31 - 0.08$ $0.51 + 0.00$	$1.49 - 0.13$ $1.17 + 0.51$	$2.01 + 0.35$ $1.15 - 0.10$	$1.49 - 0.29$ $1.43 - 0.01$

Table 5: Same as Table 34, but showing average duration (in days).

Baseline \ Area	<b>FULL</b>	<b>BIT</b>	<b>SB</b>	<b>PS</b>	<b>NEBS</b>
19961 - 19992020	$32.7 + 16.2$ $214.1 - 135.8$	$2519.21 + 51.23$ $3052.31 + 7.56.2$	$3216.13 + 65.6$ $332.76 + 51.45$	$250.57 + 164.75$ $762.96 + 158.37$	$6317.05 + 227.68$ $222.084 + 12974.4$
19961 - 2020	$39.5 + 16.2$ $139.2 + 32.0$	$2018.0 + 30.16$ $3720.28 + 529.48$	$1628.45 + 74.65$ $28.67 + 73.85$	$3702.88 + 1024.00$ $55.1 + 3.1$	$3317.30 + 03.47$ $1099.29 - 2836.93$
2001 - 2020	$38.0 - 13.9$ $136.4 - 2.1$	$19.8 - 1.0$ $37.8 + 24.0$	$15.6 - 0.07$ $36.6 - 8.4$	$20.8 + 1.7$ $101.6 + 0.7$	$15.3 + 6.8$ $122.4 - 41.1$

#### 4 Discussion

We have estimated average MHW frequency, duration, and intensity near the surface and near the bottom in the Barents Sea, based on an ocean reanalysis for the period 1991-2022. Moreover, we have investigated the impact of changing climatological average period baselines length when estimating MHW statistics in the Barents Sea, based on a regional hindcast for the period 1961-2020. We found two dominating and pervasive MHW events that in the Barents Sea in the last 30 years generally experiences few, but pervasive MHWs that affected the whole region.

Previous studies of MHWs, including in the Barents Sea, have mainly focused on the ocean surface due to the availability of satellite remote sensing sea surface temperature data (e.g., Mohamed et al., 2022). Our results indicate identified significant MHW events also near the ocean bottom in the Barents Sea, exemplified by MHW events in part related to changes in sea ice conditions, and that the bottom expressions of the MHWs tend to have lower frequency and intensity but last longer duration compared to surface MHWs. Note, however, that these statistics need to be interpreted with care, especially the statistics on near-bottom MHWs due to the low number of events (5 near-bottom MHWs were detected in the Barents Sea during 1991-2022). Among other things, this severely affected the statistical significance of the trend estimates. Nevertheless, the longer duration near the bottom was more pronounced in the eastern parts of the Barents Sea, as represented by the Pechora Sea and the Northeast Basin. We have shown that, in the north-eastern Barents Sea, the ocean-bottom layer appears to have entered a

Formatted Table

Formatted: Font: Not Bold, Italic

Formatted: Font: Bold, Not Italic

Formatted: Font: Not Bold, Italic

Formatted: Font: Not Bold, Italic

Formatted: Font: Not Bold, Italic

Formatted: Font: Not Bold, Italic

Formatted: Font: Not Bold, Italic

Formatted: Font: Not Bold, Italic

Formatted: Font: Not Bold, Italic

Formatted: Font: Not Bold, Italic

Formatted: Font: Not Bold, Italic

Formatted: Font: Not Bold, Italic

Formatted: Font: Not Bold, Italic

Formatted Table

Formatted: Font: Not Bold, Italic

Formatted: Font: Not Bold, Italic

Formatted: Font: Not Bold, Italic

Formatted: Font: Not Bold, Italic

Formatted: Font: Not Bold, Italic

Formatted: Font: Not Bold, Italic

Formatted: Font: Not Bold, Italic

Formatted: Font: Not Bold, Italic

Formatted: Font: Not Bold, Italic

Formatted: Font: Not Bold, Italic

Formatted: Font: Not Bold, Italic

Formatted: Font: Not Bold, Italic

Formatted: Font: Not Bold, Italic

Formatted: Font: Not Bold, Italic

337 ~~state of permanent MHW when using a 1961–1990 baseline. Moreover, the average duration of bottom MHWs are~~  
338 ~~approximately three times longer or more than for surface MHWs in this sub-region, independent of the choice of baseline.~~  
339 ~~One likely~~The explanation for the strong MHW signal near the bottom in this area is likely the strong reduction in sea-ice  
340 formation ~~in the shallow Pechora Sea in the south-eastern Barents Sea and on the Novaya Zemlya Bank adjacent to the~~  
341 ~~Northeast Basin, nearby banks and thus a reduction in the sinking formation of cold, brine-enriched surface water. These eastern~~  
342 ~~Barents Sea area~~ is one of the regions that has experienced the largest changes in the sea-ice cover in recent decades (e.g.,  
343 Yang et al., 2016; Onarheim and Årthun, 2017) and has thus experienced a strong reduction in the formation of cold, brine-  
344 enriched bottom water. ~~Midttun (1985) observed very cold and saline water in the deeper parts of the Northeast Basin following~~  
345 ~~cold winters in the 1970s, while Lien & Trofimov (2013) reported no such bottom water following the warmer winter of~~  
346 ~~2007/08 sinking into the deeper parts of the north-eastern Barents Sea (Midttun, 1985; Lien & Trofimov, 2013).~~ Occasional  
347 presence of such cold bottom water further west in the Barents Sea, ~~adjacent to the Bear Island Trough~~, has been hypothesized  
348 to cause differences in the position of the Polar Front ~~at the bottom~~, as detected by bottom living organisms, compared ~~to~~  
349 ~~higher in the water column based on~~with hydrographic properties in the pelagic zone (Jørgensen et al., 2015). Thus, the  
350 transition indicated by bottom MHWs in the ~~north~~-eastern Barents Sea may have a profound impact on bottom fauna by  
351 allowing boreal species with less resilience to below-zero temperatures to settle.

352 Previous findings by Mohamed et al (2022), based on satellite remote sensing sea-surface temperature data, contrasted the  
353 Spitsbergen Bank area showing no trend in MHW frequency and ~~cumulative~~ duration with the Pechora Sea area showing  
354 significant trends in both frequency and duration. None of the two regions showed significant trends in MHW ~~mean~~ intensity.  
355 Our findings agree with those of Mohamed et al. (2022) that the Pechora Sea has experienced a positive trend in ~~both~~ MHW  
356 frequency ~~and not in intensity, but our results showed no significant trend in~~ and duration, at the surface. ~~However,~~ Our  
357 results indicated that there is ~~also~~ a significant, ~~positive~~ trend in MHW ~~duration-frequency~~ near the bottom ~~in the Pechora~~  
358 ~~Sea (but not in intensity and duration)~~. Moreover, our results ~~do~~ showed positive trends in both the MHW frequency and  
359 duration on the Spitsbergen Bank ~~(at the surface)~~, although we did not find a statistically significant trend in MHW intensity  
360 ~~on the Spitsbergen Bank. But our results indicated a positive trend in the MHW intensity near the bottom on the Spitsbergen~~  
361 ~~Bank. Note, H~~however, ~~that~~ the Spitsbergen Bank is also the area where the TOPAZ reanalysis shows ~~ed~~ the largest bias and  
362 RMS deviation, as well as the lowest correlation, when compared with in-situ temperature observations. Thus, we cannot draw  
363 firm conclusions whether our results for the Spitsbergen Bank area contradict the findings of Mohamed et al. (2022).

364 Our findings that the strong 2016 MHW event was preceded by stronger than average Atlantic Water inflow and anomalously  
365 weaker ocean-to-atmosphere heat loss further suggest that MHWs may become more frequent and severe in terms of intensity  
366 and duration in a future Barents Sea with continued increase in oceanic heat advection from the North Atlantic (e.g., Årthun  
367 et al., 2019) in combination with reduced ocean-to-atmosphere heat loss within the Barents Sea (e.g., Skagseth et al., 2020).



368

## 369 **5 Data availability**

370 A list of the data products utilized in this paper, along with their availability and links to their documentation, is provided in  
371 Table 1.

## 372 **6 Author contribution**

373 All authors contributed to the design, analysis, and writing of the paper.

## 374 **7 Competing interests**

375 The authors declare that they have no conflict of interest.

## 376 **8 Acknowledgements**

377 This work was funded by the Copernicus Marine Service, contract #21002L1-COP-MFC ARC-5100.

## 378 **9 References**

379 Årthun, M., Eldevik, T., and Smedsrud, L. H.: The role of Atlantic heat transport in future Arctic winter sea ice loss. *J Clim.*,  
380 32, 3327-3341, 2019

381 Cheng, L., von Schuckmann, K., Abraham, J. P., Trenberth, K. E., Mann, M. E., Zanna, L., England, M. H., Zika, J. D., Fasullo,  
382 J. T., Yu, Y., Pan, Y., Zhu, J., Newsom, E. R., Bronselaer, B., and Lin X.: Past and future ocean warming. *Nat Rev Earth*  
383 *Environ.*, 3, 776-794, 2022

384 Chiswell, S. M.: Global Trends in Marine Heatwaves and Cold Spells: The Impacts of Fixed Versus Changing Baselines. *J*  
385 *Geophys Res Oceans*, 127, e2022JC018757, 2022

386 EU Copernicus Marine Service Product: Arctic Ocean Physics Reanalysis, Mercator Ocean International [dataset],  
387 <https://doi.org/10.48670/moi-00007>, 2022.

388 [EU Copernicus Climate Service Product: ERA5 monthly averaged data on single levels from 1940 to present \[dataset\]](https://doi.org/10.24381/cds.f17050d7),  
389 <https://doi.org/10.24381/cds.f17050d7>, 2023.

390 Fossheim, M., Primicerio, R., Johannesen, E., Ingvaldsen, R. B., Aschan, M. M. and Dolgov, A. V.: Recent warming leads to  
391 a rapid borealization of fish communities in the Arctic. *Nat Clim Change*, doi: 10.1038/nclimate2647, 2015

392 Frölicher, T. L., Fischer, E. M. and Gruber, N.: Marine heatwaves under global warming. *Nature*, 560(7718), 360–364.  
393 <https://doi.org/10.1038/s41586-018-0383-9>, 2018

Field Code Changed

394 [Gammelsrød, T., Leikvin, Ø., Lien, V., Budgell, W. P., Loeng, H., and Maslowski, W.: Mass and Heat transports in the NE](#)  
395 [Barents Sea: Observations and Models, \*J. Mar. Sys.\*, 75, 56-69, doi: 10.1016/j.jmarsys.2008.07.010, 2009](#)

396 [González-Pola, C., Larsen, K. M. H., Fratantoni, P. and Beszczynska-Möller, A. \(Eds.\): ICES Report on Ocean Climate 2019-](#)  
397 [ICES Cooperative Research Reports No. 350, 136 pp., <https://doi.org/10.17895/ices.pub.7537>, 2020](#)

398 Hackett, B., Bertino, L., Alfatih, A., Burud, A., Williams, T., Xie, J., Yumruktepe, C., Wakamatsu, T., and Melsom, A.: EU  
399 Copernicus Marine Service Product User Manual for the Arctic Ocean Physics Reanalysis Product,  
400 ARCTIC\_MULTIYEAR\_PHY\_002\_003, Issue 5.15, Mercator Ocean International,  
401 <https://catalogue.marine.copernicus.eu/documents/PUM/CEMS-ARC-PUM-002-ALL.pdf>, last access: 20 June, 2023, 2022

402 Hersbach, H., Bell, B., Berrisford, P., Biavati, G., Horányi, A., Muñoz Sabater, J., Nicolas, J., Peubey, C., Radu, R., Rozum,  
403 I., Schepers, D., Simmons, A., Soci, C., Dee, D., and Thépaut, J.-N.: ERA5 hourly data on single levels from 1940 to present.  
404 Copernicus Climate Change Service (C3S) Climate Data Store (CDS), DOI: [10.24381/cds.adbb2d47](https://doi.org/10.24381/cds.adbb2d47) (Accessed on 08-09-  
405 2022), 2023

406 Hobday, A. J., Alexander, L. V., Perkins, S. E., Smale, D. A., Straub, S. C., Oliver, E. C. J., Benthuisen, J. A., Burrows, M.  
407 T., Donat, M. G., Feng, M., Holbrook, N. J., Moore, P. J., Scannell, H. A., Gupta, A. S., Wernberg, T.: A hierarchical approach  
408 to defining marine heatwaves. *Progr. Oceanogr.*, 141, 227-238, 2016

409 [Hu, S., Zhang, L., Qian, S.: Marine heatwaves in the Arctic region: Variation in different ice covers. \*Geophysical Research\*  
410 \[Letters\]\(#\), 47, e2020GL089329, <https://doi.org/10.1029/2020GL089329>, 2020](#)

411 [Huang, B., Wang, Z., Yin, X., Arguez, A., Graham, G., Liu, C., Smith, T., Zhang H.-M.: Prolonged Marine Heatwaves in the](#)  
412 [Arctic: 1982-2020. \*Geophys. Res. Lett.\*, 48, e2021GL095590, <https://doi.org/10.1029/2021GL095590>, 2021](#)

413 Husson, B., Lind, S., Fossheim, M., Kato-Solvag, H., Skern-Mauritzen, M., Pécuchet, L., Ingvaldsen, R. B., Dolgov, A. V.  
414 and Primicerio, R.: Successive extreme climatic events lead to immediate, large-scale, and diverse responses from fish in the  
415 Arctic. *Global Change Biol*, 28, 3728-3744, 2022

416 ICES: Working Group on the Integrated Assessments of the Barents Sea (WGIBAR). ICES Scientific Reports, 4:50, 235 pp.  
417 <http://doi.org/10.17895/ices.pub.20051438>, 2022

418 Jakobsen, T., and Ozhigin, V. K., [Eds.]: The Barents Sea - Ecosystem, Resources, Management: Half a century of Russian-  
419 Norwegian cooperation. 825 pp, Tapir Academic Press, Trondheim, Norway, 2011

420 Jørgensen, L. L., Ljubin, P., Skjoldal, H. R., Ingvaldsen, R. B., Anisimova, N. and Manushin, I.: Distribution of benthic  
421 megafauna in the Barents Sea: baseline for an ecosystem approach to management. *ICES J Mar Sci.*, 72(2), 595-613,  
422 doi:10.1093/icesjms/fsu106, 2015

423 Lien, V. S. and Trofimov, A. G.: Formation of Barents Sea Branch Water in the north-eastern Barents Sea. *Polar Res*, 32,  
424 18905, 2013

425 [Lien, V. S., Gusdal, Y., Albretsen, J., Melsom, A. and Vikebø, F. B.: Evaluation of a Nordic Seas 4 km numerical ocean model](#)  
426 [hindeast archive \(SVIM\), 1960-2011. \*Fisken og Havet\*, 7, 82pp., 2013](#)

427 [Lien, V. S., Gusdal, Y. and Vikebø, F. B.: Along shelf hydrographic anomalies in the Nordic Seas \(1960-2011\): Locally](#)  
428 [generated or advective signals? \*Ocean Dynam.\*, 64, 1047-1059, 2014](#)

Formatted: Font: (Default) Times New Roman, 10 pt

Formatted: Font: (Default) Times New Roman, 10 pt

Formatted: Font: (Default) Times New Roman, 10 pt

Formatted: Font: (Default) Times New Roman, 10 pt

Formatted: Font: (Default) Times New Roman, 10 pt

Formatted: Font: (Default) Times New Roman, 10 pt

Formatted: Font: (Default) Times New Roman, 10 pt, Not

Bold

Formatted: Font: (Default) Times New Roman, 10 pt, Not

Bold

Formatted: Font: (Default) Times New Roman, 10 pt

Formatted: Font: (Default) Times New Roman, 10 pt

Formatted: Font: (Default) Times New Roman, 10 pt

Formatted: Font: (Default) Times New Roman, 10 pt

Formatted: Font: (Default) Times New Roman, 10 pt

Formatted: Font: (Default) Times New Roman, 10 pt

Formatted: Font: (Default) Times New Roman, 10 pt

Formatted: Font: (Default) Times New Roman, 10 pt

Formatted: Font: (Default) Times New Roman, 10 pt, Not

Italic

Formatted: Standard, Justified, Space Before: 0 pt, After:

6 pt

Formatted: Font: (Default) Times New Roman, 10 pt

Formatted: Font: (Default) Times New Roman, 10 pt

Formatted: Font: (Default) Times New Roman, 10 pt

Formatted: Font: (Default) Times New Roman, 10 pt

Formatted: Font: (Default) Times New Roman, 10 pt

Formatted: Font: (Default) Bitstream Vera Serif

Formatted: Font: (Default) Times New Roman, 10 pt

Formatted: Font: (Default) Times New Roman, 10 pt

Formatted: Hyperlink, Font: (Default) Times New Roman, 10

pt

Formatted: Font: (Default) Times New Roman, 10 pt

Field Code Changed

429 Lien, V. S., Hjøllø, S. S., Skogen, M. D., Svendsen, E., Wehde, H., Bertino, L., Counillon, F., Chevallier, M. and Garric, G.:  
430 An assessment of the added value from data assimilation on modelled Nordic Seas hydrography and ocean transports. *Ocean*  
431 *Modell.*, 99, 43-59. doi: 10.1016/j.ocemod.2015.12.010, 2016

432 [Lien, V. S., Schlichtholz, P., Skogseth, Ø., and Vikebø, F.B.: Wind-driven Atlantic water flow as a direct mode for reduced](#)  
433 [Barents Sea ice cover. \*J. Climate\*, 30, 803-812, 2017](#)

434

435 Lind, S., Ingvaldsen, R. B. and Furevik, T.: Arctic warming hotspot in the northern Barents Sea linked to declining sea-ice  
436 import. *Nat Clim Change*, 8, 634-639, 2018

437 Marbà, N., Jordà, G., Agustí, S., Girard, C. and Duarte, C. M.: Footprints of climate change on Mediterranean Sea biota. *Front*  
438 *Mar Sci.*, 2. <https://doi.org/10.3389/fmars.2015.00056>, 2015

439 Midttun, L.: Formation of dense bottom water in the Barents Sea. *Deep-Sea Res Part A*, 32, 1233-1241, 1985

440 Mohamed, B., Nilsen, F. and Skogseth, R.: Marine Heatwaves Characteristics in the Barents Sea Based on High Resolution  
441 Satellite Data (1982-2020). *Front Mar Sci.*, 9, 821646, doi:10.3389/fmars.2022.821646, 2022

442 Oliver, E. C. J., Benthuisen, J. A., Darmaraki, S., Donat, M. G., Hobday, A. J., Holbrook, N. J., et al.: Marine heatwaves.  
443 *Annual Review of Marine Science*, 13(1), 313-342. <https://doi.org/10.1146/annurev-marine-032720-095144>, 2021

444 [Onarheim, I.H., Eldevik, T., Årthun, M., Ingvaldsen, R. B., and Smedsrud, L. H.; Skillful prediction of Barents Sea ice](#)  
445 [cover. \*Geophys. Res. Lett.\*, 42\(13\), 5364-5371, 2015](#)

446

447 Onarheim, I. H., and Årthun, M.: Toward an ice-free Barents Sea. *Geophys. Res. Lett.*, 44, 8387-8395,  
448 doi:10.1002/2017GL074304, 2017

449 Oziel, L., Baudena, A., Ardyna, M., Massicotte, P., Randelhoff, A., Sallee, J.-B., Ingvaldsen, R. B., Devred, E., and Babin,  
450 M.: Faster Atlantic currents drive poleward expansion of temperate phytoplankton in the Arctic Ocean. *Nat Commun.*, 11(1),  
451 1705, doi:10.1038/s41467-020-15485-5, 2020

452 Sakov, P., Counillon, F., Bertino, L., Lisæter, K. A., Oke, P. R., and Korabely, A.: TOPAZ4: an ocean-sea ice data assimilation  
453 system for the North Atlantic and Arctic. *Ocean Sci.*, 8(4), 633-656, 2012

454 Scannell, H. A., Pershing, A. J., Alexander, M. A., Thomas, A. C. and Mills, K. E.: Frequency of marine heatwaves in the  
455 north Atlantic and north Pacific since 1950. *Geophys Res Lett.*, 43(5), 2069-2076. <https://doi.org/10.1002/2015GL067308>,  
456 2016

457 [Schlichtholz, P.: Subsurface ocean flywheel of coupled climate variability in the Barents Sea hotspot of global warming. \*Sci.\*](#)  
458 [\*Reports\*, 9, 13692. <https://doi.org/10.1038/s41598-019-49965-6>, 2019](#)

459 [Shepovkin, A. F., and McWilliams, J. C.: The Regional Ocean Modeling System \(ROMS\): A split-explicit, free-surface,](#)  
460 [topography-following coordinates ocean model. \*Ocean Model.\*, 9, 347-404, 2005](#)

Formatted: Font: Not Bold

Formatted: Font: Not Bold

Formatted: Font: Not Bold

Formatted: Font: Not Italic

Formatted: Font: 10 pt, English (United States)

Formatted: English (United States)

Formatted: Font: 10 pt, English (United States)

Formatted: English (United States)

Formatted: Font: 10 pt, English (United States)

Formatted: English (United States)

Formatted: Font: 10 pt, English (United States)

Formatted: English (United States)

Formatted: Font: 10 pt, English (United States)

Formatted: Font: 10 pt

Formatted: Font: 10 pt

Formatted: Space After: 6 pt, Line spacing: Multiple 1.08 li

Formatted: Font: 10 pt, Not Bold

Formatted: Font: 10 pt

Formatted: Font: 10 pt

- 461 Skagseth, Ø., *et al.*: Volume and Heat Transports to the Arctic Ocean via the Norwegian and Barents Seas. In: *Arctic Subarctic*  
462 *ocean fluxes: Defining the Role of the Northern Seas in Climate*, Dickson R, Meincke J, Rhines P (Eds.), pp. 45-64, Springer,  
463 New York, 2008
- 464 Skagseth, Ø., Eldevik, T., Årthun, M., Asbjørnsen, H., Lien, V. S., and Smedsrud, L. H.: Reduced efficiency of the Barents  
465 Sea cooling machine. *Nat Clim Change*, [doi.org/10.1038/s41558-020-0772-6](https://doi.org/10.1038/s41558-020-0772-6), 2020
- 466 Smale, D. A., Wernberg, T., Oliver, E. C. J., Thomsen, M., Harvey, B. P., Straub, S. C., *et al.*: Marine heatwaves threaten  
467 global biodiversity and the provision of ecosystem services. *Nature Clim Change*, 9(4), 306–312.  
468 <https://doi.org/10.1038/s41558-019-0412-1>, 2019
- 469 Smedsrud, L.H., Esau, I., Ingvaldsen, R.B., Eldevik, T., Haugan, P.M., Li, C., Lien, V.S., Olsen, A., Omar, A.M., Otterå, O.H.,  
470 Risebrobakken, B., Sandø, A.B., Semenov, V.A. and Sorokina, S.A.: The role of the Barents Sea in the climate system. *Rev*  
471 *Geophys.*, 51, 415-449, 2013
- 472 Smedsrud, L. H., Muilwijk, M., Brakstad, A., Madonna, E., Lauvset, S. K., Spensberger, C., Born, A., Eldevik, T., Drange,  
473 H., Jeansson, E., Li, C., Olsen, A., Skagseth, Ø., Slater, D. A., Straneo, F., Våge, K., and Årthun, M.: Nordic Seas heat loss,  
474 Atlantic inflow, and Arctic sea ice cover over the last century. *Rev Geophys.*, 60, e2020RG000725, 2022
- 475 Smith, K. E., Burrows, M. T., Hobday, A. J., Sen Gupta, A., Moore, P. J., Thomsen, M., *et al.*: Socioeconomic impacts of  
476 marine heatwaves: Global issues and opportunities. *Science*, 374(6566), eabj3593. <https://doi.org/10.1126/science.abj3593>,  
477 2021
- 478 WMO 2007: *The Role of Climatological Normals in a Changing Climate* (WMO/TD-No. 1377). Geneva.
- 479 WMO 2015: *Seventeenth World Meteorological Congress* (WMO-No. 1157). Geneva.
- 480 Xie, J. P., Counillon, F., Bertino, L., Tian-Kunze, X., and Kaleschke, L.: Benefits of assimilating thin sea ice thickness from  
481 SMOS into the TOPAZ system. *Cryosphere*, 10(6), 2745-2761, 2016
- 482 Xie, J. P., Raj, R. P., Bertino, L., Samuelsen, A., and Wakamatsu, T.: Evaluation of Arctic Ocean surface salinities from the  
483 Soil Moisture and Ocean Salinity (SMOS) mission against a regional reanalysis and in situ data. *Ocean Sci.*, 15(5), 1191-1206,  
484 2019
- 485 Xie, J. P., and Bertino, L.: EU Copernicus Marine Service Quality Information Document for the Arctic Ocean Physics  
486 Reanalysis Product, ARCTIC\_MULTITYEAR\_PHY\_002\_003, Issue 1.2, Mercator Ocean International,  
487 <https://catalogue.marine.copernicus.eu/documents/QUID/CMEMS-ARC-QUID-002-003.pdf>, last access: 20 June 2023, 2022
- 488 Xie, J. P., Raj, R. P., Bertino, L., Martinez, J., Gabarro, C., and Catany, R.: Assimilation of sea surface salinities from SMOS  
489 in an Arctic coupled ocean and sea ice reanalysis. *Ocean Sci.*, 19(2), 269-287, 2023
- 490 Yang, X.-Y., Yuan, X. and Ting, M.: Dynamical link between the Barents-Kara sea ice and the Arctic Oscillation. *J. Clim.*,  
491 29, 5103-5122. doi: 10.1175/JCLI-D-15-0669.1, 2016

Formatted: Space After: 6 pt, Line spacing: Multiple 1.08 li